AIP | The Journal of Chemical Physics

The structure and IR signatures of the arginine-glutamate salt bridge. Insights from the classical MD simulations

M. V. Vener, A. V. Odinokov, C. Wehmeyer, and D. Sebastiani

Citation: The Journal of Chemical Physics **142**, 215106 (2015); doi: 10.1063/1.4922165
View online: http://dx.doi.org/10.1063/1.4922165
View Table of Contents: http://scitation.aip.org/content/aip/journal/jcp/142/21?ver=pdfcov
Published by the AIP Publishing

The structure and IR signatures of the arginine-glutamate salt bridge. Insights from the classical MD simulations

M. V. Vener,[1,a)] A. V. Odinokov,[2] C. Wehmeyer,[3] and D. Sebastiani[4]
[1]*Mendeleev University of Chemical Technology, Moscow, Russia*
[2]*Photochemistry Center of the Russian Academy of Sciences, Moscow, Russia*
[3]*Free University, Berlin, Germany*
[4]*Martin-Luther-Universität Halle-Wittenberg, Halle, Germany*

(Received 7 March 2015; accepted 26 May 2015; published online 5 June 2015)

Salt bridges and ionic interactions play an important role in protein stability, protein-protein interactions, and protein folding. Here, we provide the classical MD simulations of the structure and IR signatures of the arginine (Arg)–glutamate (Glu) salt bridge. The Arg-Glu model is based on the infinite polyalanine antiparallel two-stranded β-sheet structure. The 1 μs *NPT* simulations show that it preferably exists as a salt bridge (a contact ion pair). Bidentate (the end-on and side-on structures) and monodentate (the backside structure) configurations are localized [Donald *et al.*, Proteins **79**, 898–915 (2011)]. These structures are stabilized by the short $^{+}$N–H$\cdots$O^{-} bonds. Their relative stability depends on a force field used in the MD simulations. The side-on structure is the most stable in terms of the OPLS-AA force field. If AMBER ff99SB-ILDN is used, the backside structure is the most stable. Compared with experimental data, simulations using the OPLS all-atom (OPLS-AA) force field describe the stability of the salt bridge structures quite realistically. It decreases in the following order: side-on > end-on > backside. The most stable side-on structure lives several nanoseconds. The less stable backside structure exists a few tenth of a nanosecond. Several short-living species (solvent shared, completely separately solvated ionic groups ion pairs, etc.) are also localized. Their lifetime is a few tens of picoseconds or less. Conformational flexibility of amino acids forming the salt bridge is investigated. The spectral signature of the Arg-Glu salt bridge is the IR-intensive band around 2200 cm^{-1}. It is caused by the asymmetric stretching vibrations of the $^{+}$N–H$\cdots$O^{-} fragment. Result of the present paper suggests that infrared spectroscopy in the 2000–2800 frequency region may be a rapid and quantitative method for the study of salt bridges in peptides and ionic interactions between proteins. This region is usually not considered in spectroscopic studies of peptides and proteins. © *2015 AIP Publishing LLC.* [http://dx.doi.org/10.1063/1.4922165]

I. INTRODUCTION

The relative importance of salt bridges or contact ion pairs in stabilizing protein structure is based on experimental results,[1–4] database studies,[3,5–7] and theoretical modeling.[8–10] There is evidence that salt bridges play a key role in opening and closing of at least certain classes of ion channels which are membrane proteins that control entry and exit of potassium and sodium to and from cells.[11,12] The salt bridge can be defined as an interaction between two groups of opposite charges in which at least one pair of heavy atoms, usually O and N, is within hydrogen bond (H-bond) distance.[13] Salt bridges (or contact ion pairs) are characterized by the short O$\cdots$N distances (<3 Å)[14,15] and are often formed in protein secondary structural elements due to side chain–side chain interactions.[6] In particular, salt bridges stabilize α-helical structures[16–20] and β-sheets.[21–23] About 40% of ion-pairs within proteins involve arginine–carboxylate interactions,[24,25] e.g., the arginine–glutamate (Arg–Glu) and arginine–aspartate side-chain interactions. By extracting orientation information from protein coordinate data,[14] in comparison with the results of quantum mechanical calculations,[26] several structures of the Arg–Glu salt bridge were postulated. The side-on and end-on structures (Fig. 1 in Ref. 13) are bidentate configurations involving formation of a ring of six heavy atoms. These structures have been observed experimentally and predicted to be the lowest energy states based on quantum mechanical calculations.[26] An additional structure, termed as "backside," is a monodentate configuration with respect to the oxygen engaging the Nη1 hydrogens closest to Nε (Fig. 1 in Ref. 13). According to a systematic geometric analysis of the Brookhaven Protein Data Bank, the stereochemistry of the side-chain H-bonds of proteins was pointed out to be characterized by at least three factors: (a) the electronic configuration of the H-bond acceptor atoms, (b) the steric accessibility of the H-bond donor atoms, and (c) the conformation of amino acid side-chains.[27]

There have also been a number of theoretical studies aimed at quantifying the strength of interaction of small ions,[9,15,26,28–37] mimicking the salt bridges between the CO_2^- side group of glutamate or asparate and the guanidinium side group of the arginine. In particular, the interaction energy in the Arg–Glu salt bridge varies from 35 to 46

a)Author to whom correspondence should be addressed. Electronic mail: mikhail.vener@gmail.com

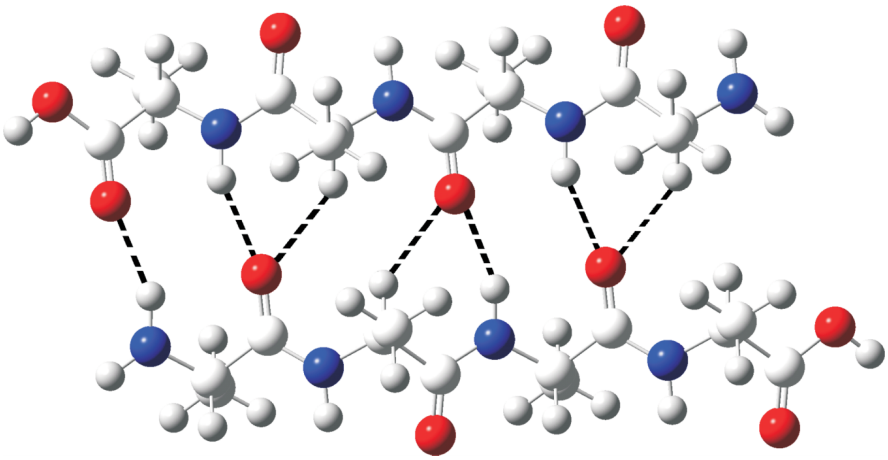

FIG. 1. The infinite alanine-based β-sheet model. The interstrand N–H···O H-bonds and C–H···O contacts are given by the broken lines. Red circles represent oxygen atoms, blue circles nitrogen atoms, large white circles carbon atoms, and small white circles hydrogen atoms. For the sake of simplicity, the terminal N and O atoms are saturated with H.

kJ/mol.[32–35] Such energies are typical for relatively strong N–H···O bonds.[38] The *end-on* and *side-on* structures are indistinguishable in the small-ions model due to the absence of side chains. A plenty of classical MD simulations on salt bridges in folded peptides do exist, e.g., see Refs. 39–44. These papers are usually focused on the solvation thermodynamics of salt bridges and backbone conformational propensities of proteins. The salt bridge stability in model peptides was studied by the DFT-based Born-Oppenheimer and classical MD simulations.[45–49] The IR spectrum was evaluated in some papers;[45,49] however, the 2000–2800 frequency region was not considered. The quantum chemistry/molecular mechanics models explore more reliable peptide structures, e.g., see Refs. 50–55. The main attention was paid to a proton transfer phenomenon in a protein environment. The IR spectra were evaluated to characterize the structure and spectroscopic signature of the simplest proton hydrates.[51,52,54] A few water molecules usually included into the quantum-chemistry part of the peptide models.[54] That is why, the considered models are hardly applicable to description of the salt bridges.

The aim of the paper is twofold: (1) To create a salt-bridge model that is free of the disadvantages of the models used in the literature and to describe the structure of Arg–Glu salt bridge at the atomic level and (2) to reveal its IR signatures using the classical MD simulations. Due to the use of classical force fields, the obtained results are semi-quantitative. It should be noted that the description of water H-bond dynamics[56,57] and proton transfer[58–60] is beyond the scope of the present paper.

II. PEPTIDE MODELS

In the present study, the infinite polyalanine antiparallel two-stranded β-sheet structure is used.[61] It was created earlier using the structure of the infinite β-sheet.[62] The two chains of the Ala peptide interact by the interstrand N–H···O H-bonds and C–H···O contacts, see Fig. 1. Their energies equal to 17 and 14 kJ/mol, respectively.[61] At the next step, the Ala peptide was modified by lysine (Lys) and glutamic acid (Glu) residues and the Lys–Glu model was obtained.[63] Finally, the lysine residue was substituted by Arg and the Arg–Glu model was created (Scheme 1).

III. COMPUTATIONAL DETAILS

The peptide is periodic along the Z-axis. The box size along this axis is defined by the length of the relaxed gas-phase β-sheet.[61,63] It equals to 14 Å. The optimal values of the box sizes along the X and Y axis are found after *NPT* equilibration of the periodic peptide solvated by 200 water molecules, see below. The topology of the periodic solute is created in two steps. At the first step, the topology file of the target tetrapeptides is prepared using the GROMACS code.[64–67] The terminal N(–H) and C(=O) atoms of the tetrapeptide backbone are not saturated by H atoms. At the second step, the bond between the terminal N(–H) atom and the image of the C(=O) atom in the neighbor cell as well as the corresponding "pairs," "angles," and "dihedrals" values[68] are defined. The "periodic_molecules" option is used in the consecutive computations. To simulate infinite peptides with 200 water molecule, we use the OPLS all-atom (OPLS-AA) force field[69,70] together with the simple point charge (SPC) and extended SPC (SPC/E) water models[71] as implemented in the GROMACS software.[67] To check the sensitivity of the results to force fields, the AMBER ff99SB-ILDN force field[72] together with the TIP3P water model[73] is also considered. The equations of motion are integrated using the leap-frog algorithm with a time step of 1 fs. Simulations are performed at the constant temperature of 298 K employing the Berendsen thermostat[74] with the time constant of 0.5 ps. An atmospheric pressure of 1 bar is maintained by the Parrinello-Rahman barostat[75] with the coupling constant of 0.5 ps. To treat long-range electrostatic interactions, the particle mesh Ewald method[76] is used. Both electrostatic and van der Waals interactions are truncated at 7 Å.

The two models are considered in the present study: Ala and Arg–Glu. Equilibration of each model performed for 1 μs in the *NPT* ensemble using the OPLS-AA force field

$$\begin{bmatrix} -\mathrm{Ala}-\mathrm{Ala}-\mathrm{Glu}-\mathrm{Ala}- \\ -\mathrm{Ala}-\mathrm{Xxx}-\mathrm{Ala}-\mathrm{Ala}- \end{bmatrix}_n$$

SCHEME 1. The periodic model mimicking the polar side-chains interaction. Ala, Glu, Lys, and Arg stand for the alanine, glutamic acid, lysine, and arginine, respectively, Xxx = Lys or Arg.

together with the SPC water model is used. *NPT* simulations are then performed for 1 μs using different force fields (OPLS-AA, AMBER) and water models (SPC, SPC/E, and TIP3P). The first 100 ns of these calculations are treated as the non-equilibrium part, while the other 900 ns are regarded as the production run and data collecting are performed every 2 ps. The "semi-isotropic" option with standard compressibility for water is used. The average values of the box sizes are 24.5, 20.0, and 14.0 Å. The distance from the ionic groups to the nearest atom from the adjacent cell along the X and Y directions is around 10 Å. It is larger than the value of the electrostatic and van der Waals cutoff (7 Å) used in the present study. Thus, the ionic groups do not interact with the opposite-charged ions from the next cells along the X and Y directions.

Obtained values of the box sizes are used in the *NVT* simulations of the infinite peptide dipole moment. A time step is 0.5 fs, and the trajectory length is 100 ps. The components of the dipole moment of the peptide are extracted from the trajectory using the "g_dipoles" Gromacs tool. The IR spectrum is obtained from the Fourier transform of the autocorrelation function of the classical dipole moment $\mathbf{M}$[77] using

$$I(\omega) = \left(\frac{2\pi\omega}{\varepsilon_0 chn}\right) F(\omega)\mathrm{Re}\int_0^\infty e^{i\omega t}\,\langle \mathbf{M}(t)\mathbf{M}(0)\rangle\, dt, \quad (1)$$

where $I(\omega)$ is the relative IR absorption at frequency ω, c is the speed of light in vacuum, ε_0 is the dielectric constant of the vacuum, n is the refractive index, which is treated as constant, and $F(\omega)$ is a quantum correction factor. Different suggestions exist for the particular shape of $F(\omega)$.[78,79] The "harmonic" quantum correction factor seems to agree better with experimental data for molecular crystals with strong H-bonds, see, e.g., Fig. 2 in Ref. 80 and is therefore used for the spectra reported below. A classical MD simulation gives a reasonable description of the IR spectrum of the liquid systems,[81,82] where a 0.5 fs time step is sufficient to produce reliable IR results for the ~2000 cm^{-1} region.[83]

IV. RESULTS

The distance between the two strands is practically constant during the MD simulations in the considered peptide models. This is due to the two reasons: (i) The use of the periodic model of peptide. (ii) The interstrand N–H···O bonds and C–H···O contacts (Fig. 1). According to quantum calculations of the cluster and infinite antiparallel β-sheet models,[61,84,85] the N–H···O bonds are stronger than the C–H···O contacts in the considered structures but only by a relatively small margin. The specific feature of the created peptide models is the fixed distance between the C_α atoms of the interacting polar side chains. It equals to ~8 Å.

A. Salt-bridge structures

During the 1 μs *NPT* simulations, the ionic groups of the Arg–Glu model spend a long time quite close to each other (Fig. 2). In accord with the literature,[81,86] the SPC and SPC/E models lead to similar results. The distance R between the central quanidino carbon and the carbon atom of the CO_2^- group is around 4.0 Å the most of the time. R ~ 3.9 Å corresponds to the *end-on* and *side-on* structures of the Arg–Glu salt-bridge (Fig. 3). They exist in a bidentate configuration involving the formation of a ring of six heavy atoms.[13,26] It is stabilized by the two $^+$N–H···O$^-$ bonds which are practically linear, the NHO angle >160°. The N···O distances vary around ~2.7 Å. These values of the N···O distances are in line with the results obtained from high-resolution protein structural analyses of the Arg–CO_2^- complexes; the majority is within 2.6 and 3.0 Å.[14] *Ab initio* computations give ~2.7 Å for the N···O distances in the formic acid-guanidinium ion pair in polar solvent.[34] Thus, these $^+$N–H···O$^-$ bonds may be treated as the short (strong)

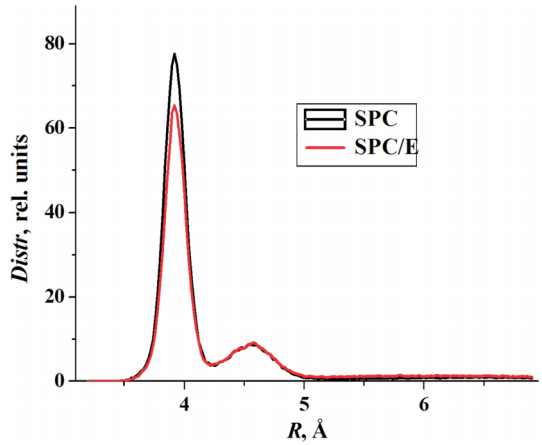

FIG. 2. The distance R between the central quanidino carbon and the carbon atom of the CO_2^- group in the Arg–Glu model obtained from the 1 μs *NPT* simulations using the OPLS-AA force field together with the SPC and SPC/E water models.

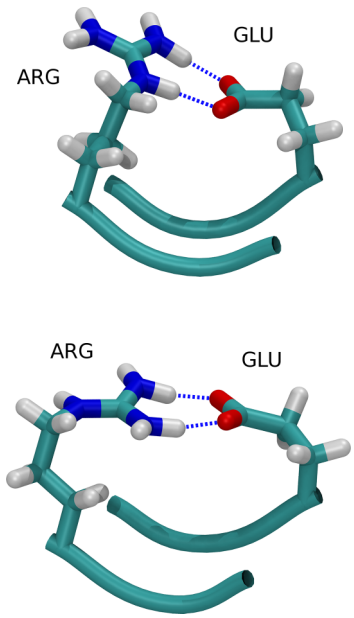

FIG. 3. Bidentate configurations of the Arg–Glu salt bridge. Upper panel: the side-on structure and lower panel: the end-on structure. The sequence of amino acid residues in the backbones is defined in Scheme 1. H-bonds between the ionic groups are denoted by the broken lines.

H-bonds.[38,87] The R value of 3.9 Å (Fig. 2) agrees nicely with the corresponding distance in the guanidinium-acetate contact ion pair in water obtained by means of MD free energy calculations[9,29,35] and classical MD simulations.[31,36] According to these papers, the global minimum of potential of mean force of guanidinium and acetate in water exists at $R \sim 3.9$ Å (the N···O distance around ~2.7 Å). The global-minimum is associated with the bidentate configurations. It should be noted that the *end-on* and *side-on* structures are indistinguishable in the small-ions model due to the absence of side chains.

Significant occurrence of R values around 4.6 Å is also observed (Fig. 2). This value corresponds to the *backside and N-epsilon* structures (Fig. 4). They exist in a monodentate configuration.[13] In contrast to the bidentate configurations, the CO_2^- group and guanidinium fragment do not arrange in same plane in the monodentate configurations, cf. Figs. 3 and 4. The N-epsilon structure is stabilized by a single short linear $^+$N–H···O$^-$ bond (the N···O distances is ~2.7 Å). The specific feature of the backside structure is a bifurcated H-bond which is formed by an oxygen atom of the CO_2^- group (Fig. 4). Our simulations highlight two important issues. (i) The use of the N···O distance in potential of mean force evaluation of guanidinium and acetate in water does not allow discriminating the bidentate and monodentate structures. (ii) The backside and N-epsilon structures are indistinguishable in the guanidinium-acetate complex.

A small minimum exists around 6.5 Å (Fig. 2). It corresponds to the solvent shared ion pair (Fig. 5). This R value agrees nicely with the corresponding distance in the guanidinium-acetate contact ion pair in water obtained by means of MD free energy calculations[9,29,35] and classical MD simulations.[31,36] According to these papers, the local minimum of potential of mean force of guanidinium and acetate in water

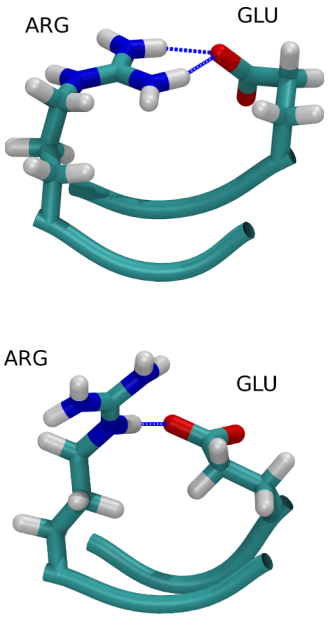

FIG. 4. Monodentate configurations of the Arg–Glu salt bridge. Upper panel: the backside structure and lower panel: the N-epsilon structure. The sequence of amino acid residues in the backbones is defined in Scheme 1. H-bonds between the ionic groups are denoted by the broken lines.

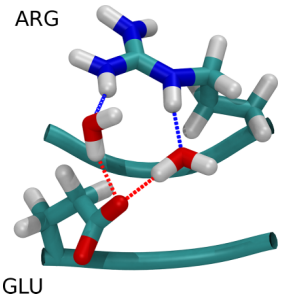

FIG. 5. The solvent shared ion pair of the Arg–Glu salt bridge. The sequence of amino acid residues in the backbones is defined in Scheme 1. The H-bonds are given by the broken lines.

exists at $R \sim 6.5$ Å. This value corresponds to the N···O distance around ~4.5 Å. The local minimum is associated with solvent shared and solvent separated ion pairs.[9,29,31,35,36]

Relative stability of the considered species is estimated using their characteristic lifetime values, evaluated from the analysis of the 1 μs *NPT* trajectory evaluated using the OPLS-AA force field together with the SPC and SPC/E water models. The relative stability decreases in the following order:

$$\text{side-on} > \text{end-on} > \text{backside} > \text{N-epsilon}. \qquad (2)$$

This result agrees nicely with the literature. According to[26] the "side-on" and "end-on," doubly N–H···O bond configurations are the most favorable, with the side-on being slightly lower in energy. The most stable side-on structure lives several nanoseconds, while the end-on structure—around a nanosecond. The backside structure lives a few tenths of a nanosecond. This observation shows that the three structures can be treated as the long-live species for which the IR spectrum can be evaluated. The less stable N-epsilon structure exists a few tens of picoseconds, while the solvent shared ion pair lives a few picoseconds. The latter two structures can be treated as the short-living species.

Sometimes, the structure with the non-interacting side chains (the completely separately solvated ionic groups) appears, see Fig. S1.[88] Quite rarely ionic groups interact with their images from the next cell along the Z direction. Such "inverted" end-one structure of the Arg–Glu salt bridge is given in Fig. S2.[88] The probability of formation of such structures is extremely small (Fig. S3[88]). The completely separately solvated ionic groups and the inverted salt bridges live for a very short period of time, one-tenth of a picoseconds or less.

To check the sensitivity of the obtained results to force fields, the 1 μs *NPT* simulations are conducted with the AMBER force field together with the TIP3P water model. Computed distribution function differs strongly from the one evaluated using the OPLS-AA force field together with the SPC and SPC/E water models, cf. Figs. 6 and 2. Most of the time, the salt bridge exists in the monodentate configuration, $R \sim 4.5$ Å (Fig. 6). This result conflicts with the available literature data.[13,26] We conclude that the AMBER force field together with the TIP3P water model should be used with caution for the description of the Arg-Glu salt bridge model created in the present study.

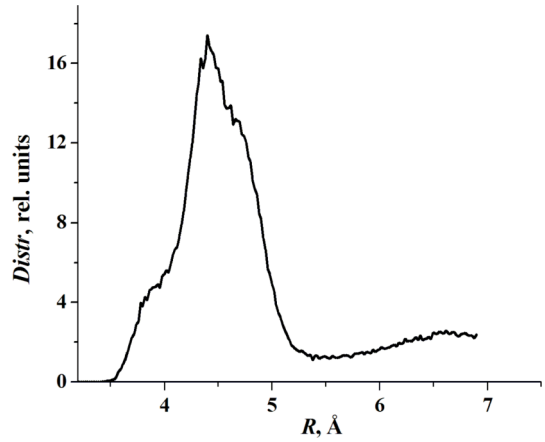

FIG. 6. The distance R between the central quanidino carbon and the carbon atom of the CO_2^- group in the Arg–Glu model obtained from the 1 μs *NPT* simulations using the AMBER force field together with the TIP3P water models.

B. Mutual position and orientation of the Arg and Glu residues and conformational flexibility of amino acids forming the salt bridge

Let us introduce a two-dimensional conformational coordinate that describes mutual position and orientation of the Arg and Glu residues. Glutamate has two equivalent oxygen atoms with indexes 1 and 2. If $r_{i\varepsilon}$ and $r_{i\eta}$ are the distances between oxygen i and N_ε or N_η atom of arginine, correspondingly, then a new composite quantities can be defined,

$$r_1 = \begin{cases} -r_{1\varepsilon}, & r_{1\varepsilon} < r_{1\eta}, \\ r_{1\eta}, & r_{1\varepsilon} \geq r_{1\eta}, \end{cases} \qquad r_2 = \begin{cases} -r_{2\varepsilon}, & r_{2\varepsilon} < r_{2\eta}, \\ r_{2\eta}, & r_{2\varepsilon} \geq r_{2\eta} \end{cases}. \tag{3}$$

Disregarding difference in Lennar-Jones parameters between ε and η nitrogen atoms, we can conclude that the distance between nitrogen atoms of arginine and oxygen atoms of glutamate cannot be less than some limiting value r_0. Then, we introduce modified coordinates,

$$r_1' = \begin{cases} -r_0 \left[\dfrac{1}{1 - r_0 - r_1} \right], & r_1 < 0, \\ r_0 \left[\dfrac{1}{1 - r_0 + r_1} \right], & r_1 \geq 0, \end{cases}$$
$$r_2' = \begin{cases} -r_0 \left[\dfrac{1}{1 - r_0 - r_2} \right], & r_2 < 0, \\ r_0 \left[\dfrac{1}{1 - r_0 + r_2} \right], & r_2 \geq 0 \end{cases}. \tag{4}$$

Taking symmetry into account, we can write the final pair of coordinates that will be used to describe salt bridge conformation further in the text,

$$\rho_1 = \frac{1}{\sqrt{2}} (r_1 + r_2),$$
$$\rho_2 = \frac{1}{\sqrt{2}} |r_1 - r_2|. \tag{5}$$

The first peak of the radial distribution function between nitrogen and oxygen atoms is confined between boundary values r_0 and r_{max}. We assume that a H-bond exists if the distance between donor and acceptor is within these limits.

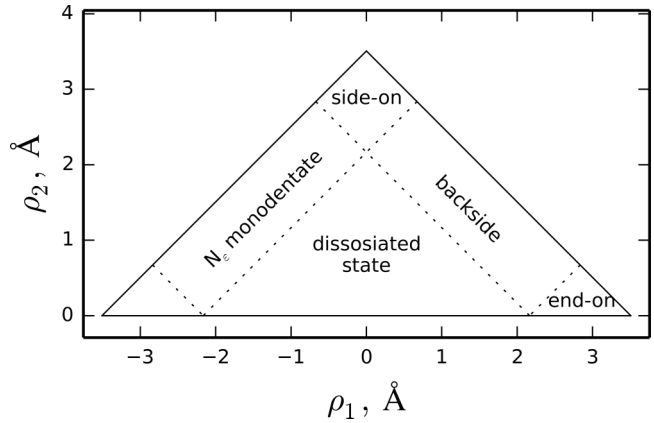

FIG. 7. Location of the different salt bridge conformations plotted in the (ρ_1,ρ_2) plane.

Thus, every configuration of the peptide may be linked to a particular region in the (ρ_1,ρ_2) plane. These regions are presented in Fig. 7. This approach provides a solid geometrical criterion to distinguish between different salt bridge conformations. A content of every conformation can be derived from the sum of hits in the corresponding region in the (ρ_1,ρ_2) plane.

A projection of the MD trajectory on the (ρ_1,ρ_2) plane for every force field is given in Fig. 8. The relative contributions of the different structures in the total ensemble of salt bridge configurations are given in Table I. The difference between AMBER and OPLS force fields is clearly seen. In the latter case, the most stable associated state corresponds to side-on structure, while in the former case, it is rare. Two hypotheses can be proposed to explain this behavior. First, the difference in parameters for covalent bonds, angles, and dihedral angles can affect the relative stability of the side chain conformations. To test this, the AMBER99SB force field was used with and without ildn corrections for dihedral angles. The results in Table I are almost the same for the both cases. It implies that the intramolecular interactions are not very important. The second possible reason is the difference in the intermolecular interactions between atoms of arginine and glutamate. Among direct interactions governed by atomic charges and Lennard-Jones parameters, the effective salt bridge stability is also affected by the water model. Two water models (SPC and

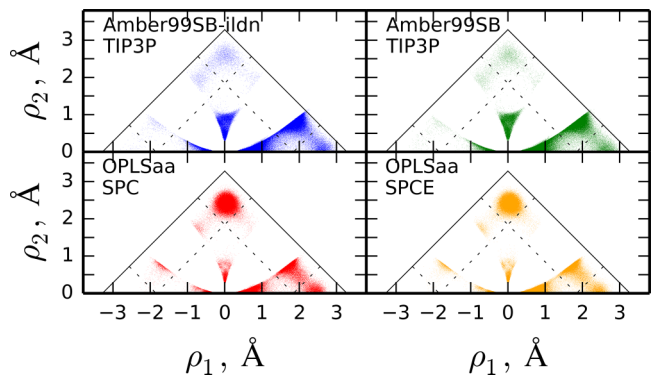

FIG. 8. Salt bridge conformations plotted in the (ρ_1,ρ_2) plane. Total amount of data points is 100 000 for each subplot.

TABLE I. The relative contributions of the different structures in the total ensemble of salt bridge configurations evaluated using different force fields (OPLS-AA, AMBER) and water models (SPC, SPC/E, TIP3P).

	Side-on	End-on	Backside	N_ε	Dissociated
OPLS-AA/SPC	44.1%	4.2%	15.0%	1.5%	35.2%
OPLS-AA/SPCE	38.0%	3.3%	14.8%	1.6%	42.3%
AMBER99SB-ildn/TIP3P	1.2%	3.4%	43.5%	0.6%	51.3%
AMBER99SB/TIP3P	1.1%	3.1%	44.0%	0.5%	51.3%

SPC/E) were used with the same force field for protein (OPLS-AA) showing measurable difference in Table I, however, this distinction can be regarded as a minor effect.

Conformational flexibility of amino acids forming the salt bridge is provided by rotation around the covalent bonds that make up the side chains (Fig. 9). For simplicity, the results obtained with the OPLS-AA force field together with the SPC water model will be considered below. The ϕ_1 and ϕ_4 angles slightly vary during the MD simulations. Thus, the conformation of the system is determined by the ϕ_2, ϕ_3, ϕ_5, and ϕ_6 torsional angles. The autocorrelation function is evaluated for these variables. The characteristic time of its fall is relatively large for ϕ_2 (3.6 ns) and ϕ_6 (5.0 ns) and much less for ϕ_3 (0.79 ns) and ϕ_5 (0.43 ns). To visualize the distribution density of states of the system in the configuration space is convenient to divide the four torsional angles into two pairs. The bidentate configuration exists at $\phi_2 = 75°$ and $\phi_6 = 100°$ (Fig. 10). It accounts for about 90% of the distribution. The solvent shared and other short-live species occur at $\phi_2 = 300°$ and $50° < \phi_6 < 300°$ in 89% of cases. The monodentate conformation exists in both these areas. It is in a dynamic equilibrium with the bidentate configuration and dissociated structures due to fluctuations of the side-chain internal coordinates within one torsion minimum, leading to breakage and formation of H-bonds.

C. IR spectrum

To achieve convergence of the IR intensities, the resulted vibrational spectrum of the Arg–Glu model is obtained after averaging over 3 spectra of the side-on, end-on, and backside structures. The IR spectrum of the particular structure is evaluated using the 100 ps *NVT* simulations (Sec. III). The dipole correlation functions, see Eq. (1), are shown in Fig. S4.[88] They are well converged and depend on specific groups.

Computed anharmonic IR spectra of the Arg–Glu and Ala models are given in Fig. 11. Three groups of bands around 1700, 1500, and 1200 cm^{-1} exist in the IR spectrum of the Ala model. They may be assigned to amide I, amide II, and amide III vibrations.[89] Their frequencies and relative IR intensities are in reasonable agreement with the available experimental data.[89,90] Amide I vibrations of the Arg–Glu model are very close to those of the Ala model. Amide II and III vibrations of the Arg–Glu model are less intensive and very noisy. The two doubles of the IR-intensive bands around 3400 and 3200 cm^{-1} may be assigned to amide A and B bands, respectively.[89] The frequencies and IR intensities of these bands are very similar for the both peptides and caused by the stretching vibrations of the NH groups of the polypeptide backbone. The band around 3600 cm^{-1} of the Arg-Glu model may be assigned to the stretching vibrations of the guanidinium NH groups, which do not involve into formation of the H-bonds with the CO_2^- group (Figs. 3 and 4). The bands in the 2800–2500 cm^{-1} frequency region can be tentatively assigned to some combined vibrations. Such bands do exist in the IR spectrum of the crystalline polyalanine[90] and crystallosolvates of aminoacids.[91,92] The band around 2200 cm^{-1} is caused by the asymmetric stretching vibrations of the $^+N–H\cdots O^-$ bond.

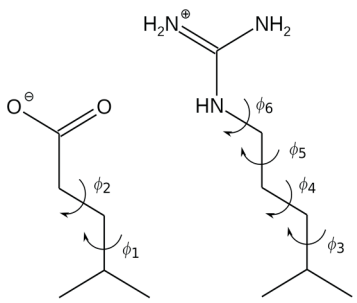

FIG. 9. Torsional angles defining the conformations of the glutamate and arginine side chains.

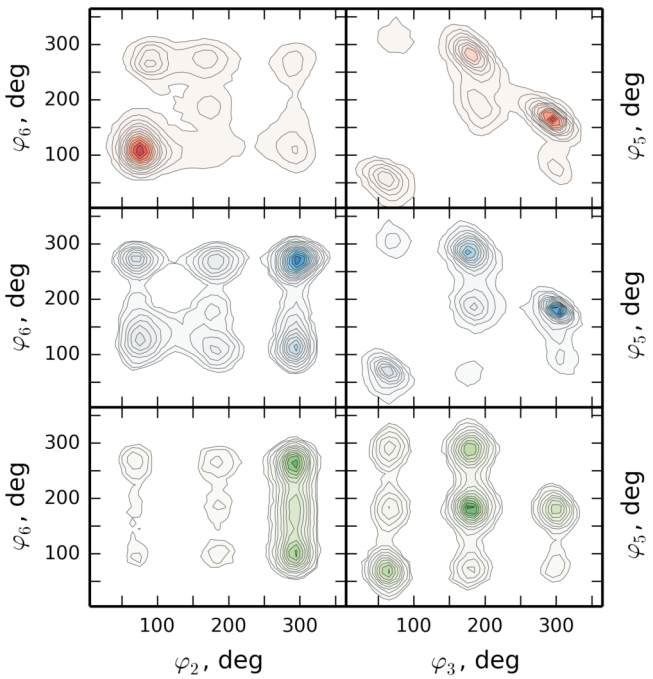

FIG. 10. The density distribution of the system in the configuration space defined by a certain pair of torsion angles: ϕ_2, ϕ_6 and ϕ_3, ϕ_5. Upper panel: the bidentate configuration. Middle panel: the monodentate configuration. Lower panel: the solvent shared and other short-live species. For convenience, the normalization of the distribution function is the same for considered structures. The non-linear color scale is used.

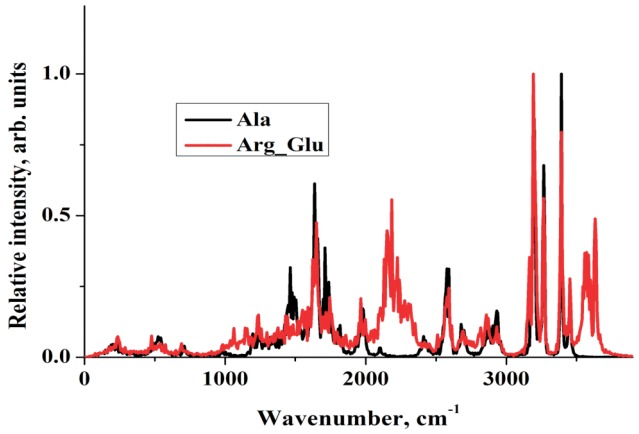

FIG. 11. Computed anharmonic IR spectrum of the peptide models with (Arg–Glu, red line) and without (Ala, black line) polar residues.

The intense band near 2400 cm^{-1} exists in the IR spectra of solid 1:1 pyridine-benzoic acid complexes[93] and is associated with the strong (short) N···H+···O bond.[87]

The computed IR spectra of the side-on, end-on, and backside structures of the Arg–Glu salt bridge are very close to each other. The point is that the three spectra are characterized by the IR-intense band around 2200 cm^{-1}. This result can be explained as follows. According to[94,95] the frequency of the OH/NH stretching vibration defined by the distance between the heavy atoms forming the H-bonded fragment. The O···N distance is very close in the considered structures. This observation shows that the spectral signature of the Arg–Glu salt bridge is the IR-intensive band around 2200 cm^{-1}.

To check the sensitivity of the vibrational spectrum to force fields and water models, the IR spectrum of the Arg–Glu model is evaluated using the OPLS-AA force field together with the SPC/E water model and the AMBER force field together with the TIP3P water model. For the sake of comparison, the backside structure is considered. The computed IR spectrum is given in Fig. 12. The SPC and SPC/E water models give the similar IR spectra, which differ strongly from the one evaluated using the TIP3P model. In our opinion, the differences in the high-frequency region is caused by the fact that the AMBER force field together with

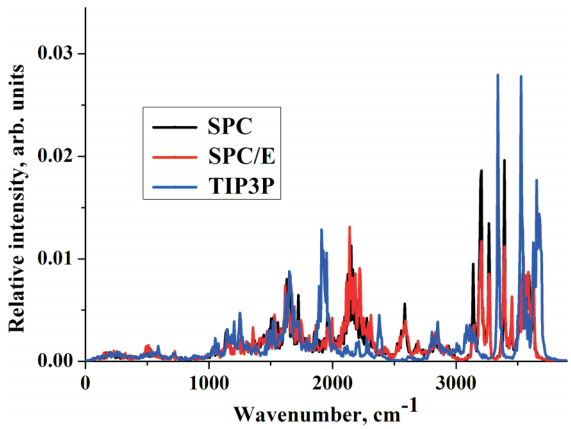

FIG. 12. Computed anharmonic IR spectrum of the backside structure evaluated using the OPLS-AA force field together with the SPC and SPC/E water models and the AMBER force field together with the TIP3P water model.

the TIP3P water model underestimates the H-bond energy between the guanidinium NH groups and water molecules in comparison with the corresponding energies evaluated using the OPLS-AA force field. On the other hand, the AMBER force field overestimates stability of the backside structure. As a result, the too short $^{+}N–H\cdots O^{-}$ bond appears and the band, associated with the asymmetric stretching vibrations of this fragment, locates below 2000 cm^{-1} (Fig. 11). Obtained results agree with the literature data. According to Ref. 96, the main difference between the water models used in the classical MD simulations is mostly due to the different solvation of polar groups of the peptide.

The pure IR spectra of SPC water is presented in Fig. S5.[88] It gives a very rough description of the IR spectrum of the bulk water. In order to get a reliable spectrum, one has to use flexible SPC and flexible SPC/E water models.[81,82]

V. DISCUSSION

Vibrational spectroscopy has been applied for decades as a powerful probe of polypeptide and protein secondary structures.[89,97] The major attention is usually focused on the analysis of the amide I band. It is a broad band located between approximately 1700 and 1600 cm^{-1} and is a complex composite of a number of overlapping bands characteristic for specific secondary structures, such as α helix, β structure, turns, and nonordered segments, e.g., see Refs. 98–102. The salt-bridge structure is also investigated in this spectroscopic region.[37] To our best knowledge, the 2000–2800 frequency region has not been systematically used for identification of salt bridges and ionic interactions in peptides and proteins, e.g., see Refs. 103 and 104. On the other hand, the spectroscopic features of the N···H+···O bonds in gas and condensed phases have been studied experimentally and theoretically. Results of these studies are discussed below.

According to Ref. 105, the broad band at around 2500 cm^{-1} is a signature of the N···H+···O bond in the protonated N-terminus in isolated dipeptides. Similar results were obtained for protonated polyalanine peptides.[106] The band at ~2700 cm^{-1} corresponds to the charge solvating NH+ (NH+···O=C) vibration of the most stable conformer of Ala4H+ peptide. Theoretical studies of microsolvation of aminoacids by water lead to similar results. The lowest energy canonical conformers of lysine-$(H_2O)_3$[107] and arginine-(H_2O)[108] are characterized by IR intensive bands around 2600 and 2350 cm^{-1}, respectively. This band is associated with the short (strong) intermolecular N–H···O bond between the NH2 group of the amino acid and water molecule.

Two equally intense broad bands near 1930 and 2450 cm^{-1} exist in the IR spectra of solid 1:1 pyridine-benzoic acid complexes.[93] These bands were attributed to O–H/N-H stretching vibrations of the double-minimum potential function of the N···H+···O fragment. The IR band in the 2500–2600 cm^{-1} frequency region is detected for three forms of the 4-hydroxybenzoic acid:4,4′-bipyridine (2:1) co-crystal[109] and cytosine salts.[110] These crystals are characterized by the strong (short) N···H+···O hydrogen bond.

The 1700–2500 frequency region was considered in experimental and theoretical studies of protonated water

networks in bacteriorhodopsin[43,111,112] and proton pumping in biomolecular proton pumps.[54] The main attention was paid to the structure and spectroscopic signatures of the simplest proton hydrates, in particular, the $H_5O_2^+$ ion. Its specific feature is the IR intensive band near 1720 cm^{-1}.[113] The effect of proton transfer on vibrations of the short intermolecular N···H+···O bond in aprotic solvents was studied in Ref. 87. As a result of geometrical changes caused by the increase of the static dielectric permittivity from 1 to 4.9, the harmonic frequency of the O–H stretching vibration decreases from about 2500 to 2300 cm^{-1} for the 1:1 complex of 2,4,6-trimethylpyridine with 3,5-dinitrobenzoic acid.

According to the results of the present study, the spectroscopic signature of the Arg–Glu salt bridge is the IR intensive band in around 2200 cm^{-1}. The IR absorption of bulk water is practically negligible in the 1900–2900 frequency region.[114,115] Therefore, the IR band(s) of the Arg–Glu salt bridge may be detected experimentally using attenuated total reflection Fourier-transform infrared spectroscopy.

VI. CONCLUSIONS

The Arg–Glu salt bridge model is created. It is free of the disadvantages of the salt-bridge models used in the literature. Its specific features are the following. (i) A backbone conformation is fixed and the distance between the C_α atoms of the polar side chains is practically constant; (ii) conformational flexibility of the polar side chains causes the appearance of a variety of structures (bidentate and monodentate configurations, solvent shared ion pair, etc.); (iii) the number of water molecules is relatively large to describe the first and second solvation shells of the charged groups; and (iv) the size of the simulation system is appropriate for the DFT-based MD simulations.

The Arg–Glu model exists in bidentate (the side-on and end-on structures) and monodentate (the backside structure) configurations. The side-on and end-on structures are stabilized by twin short N–H···O bonds; the N···O distances is ~2.7 Å. In contrast to the bidentate configurations, the CO_2^- group and guanidinium fragment do not arrange in same plane in the backside structure. The latter is stabilized by a bifurcated H-bond which is formed by an oxygen atom of the CO_2^- group. The relative stability of the salt-bridge structures depends on the force field used in the MD simulations. The side-on structure is the most stable in terms of the OPLS-AA force field. If AMBER ff99SB-ILDN is used, the backside structure is the most stable. Compared with experimental data, simulations using the OPLS-AA force field describe the stability of the salt bridge structures quite realistically.

According to the OPLS-AA force field together with the SPC and SPC/E water models, the most stable side-on structure lives several nanoseconds, while the less stable backside structure lives a few tenths of a nanosecond. The second monodentate configuration, the N-epsilon structure, is localized. It is stabilized by the short N–H···O bond which forms by the N–H group of the N_ε atom of the guanidinium side group. The N-epsilon structure lives a few tens of picoseconds and can be treated as the short-living species. The solvent shared ion pair is also localized. Its lifetime is around a picosecond.

The IR-intensive band around 2200 cm^{-1} is found to be the spectral signature of the Arg–Glu salt bridge. We do hope that infrared spectroscopy in the 2000–2800 frequency region may be a rapid and quantitative method for the study of ionic interactions between proteins and salt bridges in peptides.

ACKNOWLEDGMENTS

M.V.V. thanks the Alexander von Humboldt foundation (a renewed research stay in Germany) and DAAD (the scholarship program "Research stays for University Academics and Scientists"). D.S. acknowledges support from the DFG Sonderforschungsbereich SFB/TRR 102. M.V.V. thanks Professor Ana-Nicoleta Bondar for useful comments.

[1]A. Horvitz, L. Serrano, B. Avron, M. Bycroft, and A. R. Fersht, J. Mol. Biol. **216**, 1031 (1990).
[2]J. M. Scholtz, H. Qian, V. H. Robbins, and R. L. Baldwin, Biochemistry **32**, 9668 (1993).
[3]C. D. Waldburger, J. F. Schildbach, and R. T. Sauer, Nat. Struct. Biol. **2**, 122 (1995).
[4]W. C. Wimley, K. Gawrisch, T. P. Creamer, and S. H. White, Proc. Natl. Acad. Sci. U. S. A. **93**, 2985 (1996).
[5]D. J. Barlow and J. M. Thornton, Biopolymers **25**, 1717–1733 (1986).
[6]S. Kumar and R. Nussinov, ChemBioChem **3**, 604–617 (2002), and references therein.
[7]A. Nayek, P. S. S. Gupta, S. Banerjee, B. Mondal, and A. K. Bandyopadhyay, PLoS One **9**, e93862 (2014).
[8]Z. S. Hendsch and B. Tidor, Protein Sci. **3**, 211 (1994).
[9]A. Masunov and T. Lazaridis, J. Am. Chem. Soc. **125**, 1722 (2003).
[10]H. Gong and K. F. Freed, Biophys. J. **98**, 470 (2010).
[11]B. Hille, C. A. Armstrong, and R. MacKinnon, Nat. Med. **5**, 1105–1109 (1999).
[12]*Computer Simulations and Modeling of Ion Channels*, edited by M. E. Green (Academic Press, New York, 1998).
[13]J. E. Donald, D. W. Kulp, and W. F. DeGrado, Proteins **79**, 898–915 (2011).
[14]J. Singh, J. M. Thornton, M. Snarey, and S. F. Campbell, FEBS Lett. **224**, 161 (1987).
[15]Z. Yu, M. P. Jacobson, J. Jasovitz, C. S. Rapp, and R. A. Friesner, J. Phys. Chem. B **108**, 6643 (2004).
[16]S. Marqusee and R. L. Baldwin, Proc. Natl. Acad. Sci. U. S. A. **84**, 8898–8902 (1987).
[17]D. Walther and P. Argos, Protein Eng. **9**, 471–478 (1996).
[18]A. G. Therien, F. E. M. Grant, and C. M. Deber, Nat. Struct. Biol. **8**, 597–601 (2001).
[19]N. Errington and A. J. Doig, Biochemistry **44**, 7553 (2005).
[20]R. P. Cheng, W.-R. Wang, P. Girinath, P.-A. Yang, R. Ahmad, J.-H. Li, P. Hart, B. Kokona, R. Fairman, C. Kilpatrick, and A. Argiros, Biochemistry **51**, 7157–7172 (2012).
[21]C. A. Blasie and J. M. Berg, Biochemistry **36**, 6218–6222 (1997).
[22]J. S. Merkel, J. M. Sturtevant, and L. Regan, Structure **7**, 1333–1343 (1999).
[23]A. Dos, V. Schimming, S. Tosoni, and H.-H. Limbach, J. Phys. Chem. B **112**, 15604 (2008).
[24]J. F. Riordan, K. D. McElvany, and C. L. Borders, Jr., Science **195**, 884 (1977).
[25]D. J. Barlow and J. M. Thornton, J. Mol. Biol. **168**, 867 (1983).
[26]J. B. O. Mitchell, J. M. Thornton, J. Singh, and S. L. Price, J. Mol. Biol. **226**, 251–262 (1992).
[27]J. A. Ippolito, R. S. Alexander, and D. W. Christainson, J. Mol. Biol. **215**, 457 (1990).
[28]R. Luo, L. David, H. Hung, J. Devaney, and M. K. Gilson, J. Phys. Chem. B **103**, 727–736 (1999).
[29]X. Rozanska and C. Chipot, J. Chem. Phys. **112**, 9691–9694 (2000).
[30]D. Frigzes, F. Alber, S. Pongor, and P. Carloni, J. Mol. Struct.: THEOCHEM **574**, 39 (2001).
[31]K. Sagarik and S. Chaiyapongs, Biophys. Chem. **117**, 119 (2005).
[32]D. J. Mandell, I. Chorny, E. S. Groban, S. E. Wong, E. Levine, C. S. Rapp, and M. P. Jacobson, J. Am. Chem. Soc. **129**, 820–827 (2007).
[33]S. Liao and M. E. Green, Comput. Theor. Chem. **963**, 207 (2011).
[34]P. I. Nagy and P. W. Erhardt, J. Phys. Chem. B **114**, 16436 (2010).
[35]O. Yuzlenko and T. Lazaridis, J. Phys. Chem. B **115**, 13674–13684 (2011).

[36]K. T. Debiec, A. M. Gronenborn, and L. T. Chong, J. Phys. Chem. B **118**, 6561 (2014).
[37]A. Huerta-Viga, S. R. Domingos, S. Amirjalayer, and S. Woutersen, Phys. Chem. Chem. Phys. **16**, 15784 (2014).
[38]T. Steiner, Angew. Chem., Int. Ed. **41**, 48 (2002).
[39]F. B. Sheinerman and B. Honig, J. Mol. Biol. **318**, 161 (2002).
[40]J. Tsai and M. Levitt, Biophys. Chem. **101**, 187 (2002).
[41]A. S. Thomas and A. H. Elcock, J. Am. Chem. Soc. **126**, 2208 (2004).
[42]G. Reddy, J. E. Straub, and D. Thirumalai, J. Phys. Chem. B **113**, 1162 (2009).
[43]K.-I. Oh, K.-K. Lee, E.-K. Park, Y. Jung, G.-S. Hwang, and M. Cho, Proteins **80**, 977 (2012).
[44]R. Salari and L. T. Chong, J. Phys. Chem. B **116**, 2561 (2012), and references therein.
[45]M. Kobus, P. H. Nguyen, and G. Stock, J. Chem. Phys. **133**, 034512 (2010).
[46]E. Pluharová, O. Marsalek, B. Schmidt, and P. Jungwirth, J. Chem. Phys. **137**, 185101 (2012).
[47]C. Rapp, H. Klerman, E. Levine, and C. L. McClendon, PLoS One **8**, e57804 (2013).
[48]A. D. White, A. J. Keefe, J.-R. Ella-Menye, A. K. Nowinski, Q. Shao, J. Pfaendtner, and S. Jiang, J. Phys. Chem. B **117**, 7254 (2013).
[49]D. Semrouni, A. Sharma, J.-P. Dognon, G. Ohanessian, and C. Clavaguéra, J. Chem. Theory Comput. **10**, 3190 (2014).
[50]Y.-S. Lee and M. Krauss, J. Am. Chem. Soc. **126**, 2225 (2004).
[51]G. Mathias and D. Marx, Proc. Natl. Acad. Sci. U. S. A. **104**, 6980 (2007).
[52]P. Phatak, N. Ghosh, H. Yu, Q. Cui, and M. Elstner, Proc. Natl. Acad. Sci. U. S. A. **105**, 19672 (2008).
[53]I. Kaliman, B. Grigorenko, M. Shadrina, and A. Nemukhin, Phys. Chem. Chem. Phys. **11**, 4804 (2009).
[54]P. Goyal, N. Ghosh, P. Phatak, M. Clemens, M. Gaus, M. Elstner, and Q. Cui, J. Am. Chem. Soc. **133**, 14981–14997 (2011).
[55]A. Paasche, T. Schirmeister, and B. Engels, J. Chem. Theory Comput. **9**, 1765 (2013).
[56]C. Rocchi, A. R. Bizzarri, and S. Cannistraro, Phys. Rev. E **57**, 3315 (1998).
[57]F. Sterpone, G. Stirnemann, J. T. Hynes, and D. Laage, J. Phys. Chem. B **114**, 2083 (2010).
[58]S. Lammers, S. Lutz, and M. Meuwly, J. Comput. Chem. **29**, 1048 (2008).
[59]M. G. Wolf and G. Groenhof, J. Comput. Chem. **35**, 657 (2014).
[60]K. L. Joshi, G. Psofogiannakis, A. C. T. van Duin, and S. Raman, Phys. Chem. Chem. Phys. **16**, 18433 (2014).
[61]M. V. Vener, A. N. Egorova, D. P. Fomin, and V. G. Tsirelson, J. Phys. Org. Chem. **22**, 177 (2009).
[62]J. Rossmeisl, J. K. Nørskov, and K. W. Jacobsen, J. Am. Chem. Soc. **126**, 13140 (2004).
[63]M. V. Vener, A. N. Egorova, D. P. Fomin, and V. G. Tsirelson, J. Mol. Struct. **972**, 11 (2010).
[64]H. J. C. Berendsen, D. van der Spoel, and R. van Drunen, Comput. Phys. Commun. **91**, 43 (1995).
[65]E. Lindahl, B. Hess, and D. van der Spoel, J. Mol. Model. **7**, 306 (2001).
[66]D. van der Spoel, E. Lindahl, D. Hess, G. Groenhof, A. E. Mark, and H. J. C. Berendsen, J. Comput. Chem. **26**, 1701 (2005).
[67]B. Hess, C. Kutzner, D. van der Spoel, and E. Lindahl, J. Chem. Theory Comput. **4**, 435 (2008).
[68]D. van der Spoel, A. R. van Bruuren, E. Apol, P. J. Meulenhoff, D. P. Tieleman, A. L. T. M. Sijbers, B. Hess, K. A. Feenstra, E. Linhdahl, R. van Drunen, H. J. C. Berendsen, and H. J. C. Gromacs, User Manual, Version 4.0.7, Groeninger, The Netherlands, 1991-2008.
[69]W. L. Jorgensen, D. S. Maxwell, and J. Tirado-Rives, J. Am. Chem. Soc. **118**, 11225 (1996).
[70]G. A. Kaminski, R. A. Friesner, J. Tirado-Rives, and W. L. Jorgensen, J. Phys. Chem. B **105**, 6474 (2001).
[71]H. J. C. Berendsen, J. R. Grigera, and T. P. Sraatsma, J. Phys. Chem. **91**, 6269 (1987).
[72]K. Lindorff-Larsen, S. Piana, K. Palmo, P. Maragakis, J. L. Klepeis, R. O. Dror, and D. E. Shaw, Proteins **78**, 1950 (2010).
[73]W. L. Jorgensen, J. Chandrasekhar, J. D. Madura, R. W. Impey, and M. L. Klein, J. Chem. Phys. **79**, 926 (1983).
[74]H. J. C. Berendsen, J. P. M. Postma, W. F. van Gunsteren, A. DiNola, and J. R. Haak, J. Chem. Phys. **81**, 3684 (1984).
[75]M. Parrinello and A. Rahman, J. Appl. Phys. **52**, 7182 (1981).
[76]U. Essmann, L. Perera, M. L. Berkowitz, T. Darden, H. Lee, and L. G. Pedersen, J. Chem. Phys. **103**, 8577 (1995).
[77]W. B. Bosma, L. E. Fried, and S. Mukamel, J. Chem. Phys. **98**, 4413 (1993).
[78]M.-P. Gaigeot and M. Sprik, J. Phys. Chem. B **107**, 10344 (2003).
[79]R. Ramirez, T. Lopez-Ciudad, P. Kumar, and D. Marx, J. Chem. Phys. **121**, 3973 (2004).
[80]M. V. Vener and J. Sauer, Phys. Chem. Chem. Phys. **7**, 258 (2005).
[81]M. Praprotnik, D. Janezic, and J. Mavri, J. Phys. Chem. A **108**, 11056 (2004).
[82]M. Praprotnik and D. Janeži, J. Chem. Phys. **122**, 174103 (2005).
[83]H. Yu and Q. Cui, J. Chem. Phys. **127**, 234504 (2007).
[84]S. Scheiner, J. Phys. Chem. B **110**, 18670 (2006).
[85]M. V. Vener, A. N. Egorova, D. P. Fomin, and V. G. Tsirelson, Chem. Phys. Lett. **440**, 279 (2007).
[86]C. T. Andrews and A. H. Elcock, J. Chem. Theory Comput. **9**, 4585 (2013).
[87]S. Kong, I. G. Shenderovich, and M. V. Vener, J. Phys. Chem. A **114**, 2393 (2010).
[88]See supplementary material at http://dx.doi.org/10.1063/1.4922165 for several figures. In supplementary figure S1, we show the completely separately solvated ionic groups of the Arg-Glu model. In Fig. S2, we indicate the inverted end-on structure of the Arg–Glu salt bridge. Figure S3 shows the distribution function of the distance between the charged groups. In Fig. S4, we indicate the dipole correlation functions evaluated using the OPLS-AA force field together with the SPC water model. Figure S5 shows IR spectrum of the bulk water evaluated using the OPLS-AA force field together with the SPC water model.
[89]A. Barth, Biochim. Biophys. Acta, Bioenerg. **1767**, 1073–1101 (2007), and references therein.
[90]S.-H. Lee and S. Krimm, Biopolymers **46**, 283–317 (1998).
[91]A. V. Churakov, P. V. Prikhodchenko, J. A. K. Howard, and O. Lev, Chem. Commun **2009**, 4224.
[92]M. V. Vener, A. G. Medvedev, A. V. Churakov, P. V. Prikhodchenko, T. A. Tripol'skaya, and O. Lev, J. Phys. Chem. A **115**, 13657 (2011).
[93]S. L. Johnson and K. A. Rumon, J. Phys. Chem. **69**, 74–86 (1965).
[94]A. Novak, Struct. Bonding **18**, 177 (1974).
[95]N. D. Sokolov, M. V. Vener, and V. A. Savel'ev, J. Mol. Struct. **222**, 365 (1990).
[96]D. Paschek, R. Day, and A. E. García, Phys. Chem. Chem. Phys. **13**, 19840 (2011).
[97]P. W. Holloway and H. H. Mantsch, Biochemistry **27**, 7991 (1988).
[98]E. H. G. Backus, R. Bloem, R. Pfister, A. Moretto, M. Crisma, C. Toniolo, and P. Hamm, J. Phys. Chem. B **113**, 13405 (2009).
[99]F. Ingrosso, G. Monard, M. H. Farag, A. Bastida, and M. F. Ruiz-Lopez, J. Chem. Theory Comput. **7**, 1840 (2011).
[100]Z.-W. Qu, H. Zhu, and V. May, J. Comput. Chem. **32**, 1500 (2011).
[101]P. Pandey, A. Pramanik, and T. Chakraborty, Chem. Phys. **389**, 88 (2011).
[102]A. Nicolaides, T. Soulimane, and C. Varotsis, Phys. Chem. Chem. Phys. **17**, 8113 (2015).
[103]M.-P. Gaigeot, Phys. Chem. Chem. Phys. **12**, 3336 (2010), and references therein.
[104]H. Zhu, M. Blom, I. Compagnon, A. M. Rijs, S. Roy, G. von Helden, and B. Schmidt, Phys. Chem. Chem. Phys. **12**, 3415 (2010).
[105]C. M. Leavitt, A. F. DeBlase, C. J. Johnson, M. van Stipdonk, A. B. McCoy, and M. A. Johnson, J. Phys. Chem. Lett. **4**, 3450 (2013).
[106]T. D. Vaden, T. S. J. A. de Boer, J. P. Simons, L. C. Snoek, S. Suhai, and B. Paizs, J. Phys. Chem. A **112**, 4608 (2008).
[107]T.-K. Hwang, G.-Y. Eom, M.-S. Choi, S.-W. Jang, J.-Y. Kim, and S. Lee, J. Phys. Chem. B **115**, 10147 (2011).
[108]S. Im, S.-W. Jang, S. Lee, Y. Lee, and B. Kim, J. Phys. Chem. A **112**, 9767 (2008).
[109]A. Mukherjee, S. Tothadi, S. Chakraborty, S. Ganguly, and G. R. Desiraju, CrystEngComm **15**, 4560 (2013).
[110]S. Chakraborty, S. Ganguly, and G. R. Desiraju, CrystEngComm **16**, 4732 (2014).
[111]F. Garczarek, J. Wang, M. A. El-Sayed, and K. Gerwert, Biophys. J. **87**, 2676 (2004).
[112]J. Coutre, J. Tittort, D. Oesterhelt, and K. Gerwert, Proc. Natl. Acad. Sci. U. S. A. **92**, 4962 (1995).
[113]M. V. Vener and N. B. Librovich, Int. Rev. Phys. Chem. **28**, 407 (2009).
[114]J. E. Bertie and Z. D. Lan, Appl. Spectrosc. **50**, 1047 (1996).
[115]T. Ikeda, J. Chem. Phys. **141**, 044501 (2014), and references therein.